

First detection of CS masers around a high-mass young stellar object, W51 e2e

ADAM GINSBURG^{1,2} AND CIRIACO GODDI^{3,4}

¹*Department of Astronomy, University of Florida, PO Box 112055, USA*

²*Jansky fellow of the National Radio Astronomy Observatory, Socorro, NM 87801 USA*

³*ALLEGRO/Leiden Observatory, Leiden University, PO Box 9513, 2300 RA Leiden, the Netherlands*

⁴*Department of Astrophysics/IMAPP, Radboud University Nijmegen, PO Box 9010, 6500 GL Nijmegen, the Netherlands*

ABSTRACT

We report the discovery of maser emission in the two lowest rotational transitions of CS toward the high-mass protostar W51 e2e with ALMA and the JVL A. The masers from CS J=1-0 and J=2-1 are neither spatially nor spectrally coincident (they are separated by ~ 150 AU and ~ 30 km s⁻¹), but both appear to come from the base of the blueshifted outflow from this source. These CS masers join a growing list of rarely-detected maser transitions that may trace a unique phase in the formation of high-mass protostars.

1. INTRODUCTION

Because of their compactness, high brightness, and ubiquity, masers are unique diagnostic probes of the early stages of star formation. Long baseline interferometric studies (e.g., Matthews et al. 2010; Goddi et al. 2011; Moscadelli & Goddi 2014; Moscadelli et al. 2016) have revealed that maser emission lines can trace accretion structures, shocks in outflows, and disk winds in the circumstellar environments of protostars.

While some chemical species, specifically CH₃OH, H₂O, and OH, are detected in hundreds of star-forming regions across the Galaxy, others are more rare, such as SiO (around young stars; SiO masers are common in evolved stars), H₂CO, and NH₃ (e.g., Goddi et al. 2009; Cho et al. 2016; Ginsburg et al. 2015; Goddi et al. 2015; Mills et al. 2018). The rarity of this latter group of masers is so far unexplained, though since they have only been detected toward high-mass star-forming regions (Araya et al. 2015; Wilson & Schilke 1993; Hofner et al. 1994; Cordiner et al. 2016), they are likely to be pumped by the strong radiation only present around high-mass protostars.

The rotational transitions of CS have been theorized to arise in some environments (Schoenberg 1988), and Highberger et al. (2000) reported a possible maser from the CS $v=1$ J=3-2 transition in IRC+10216, but no masers have been observed in the rotational transitions of the vibrational ground-state of CS.

The W51 A high-mass star-forming region (at a distance of 5.4 kpc - Sato et al. 2010) is one of the most massive and luminous ($\sim 10^7 L_{\odot}$) in the Galaxy (Ginsburg 2017), and it is host to three high-mass protostellar systems with $> 100 M_{\odot}$ hot cores, W51 IRS2/North,

W51 e2e, and W51 e8 (Ginsburg et al. 2017). Among the known high-mass protostars exhibiting maser emission, W51 IRS2/North stands out as host to some of the rarest maser transitions. It powers a large number (> 20) of rare NH₃ maser lines as well as rare SiO masers (Henkel et al. 2013; Goddi et al. 2015; Hasegawa et al. 1986; Eisner et al. 2002). W51 e2e and e8, on the other hand, are more typical high-mass star-forming region in terms of their maser emission, exhibiting only CH₃OH, H₂O, and OH masers (Goddi et al. 2016).

We have observed all three hot cores in the W51 A region in the two lowest transitions of CS, J=1-0 and J=2-1. We report here the first detection of maser emission from CS $v = 0$ in both the J=1-0 and J=2-1 transitions in W51 e2e and nondetections in the other two hot cores.

2. OBSERVATIONS

We report observations from three different observing programs: ALMA 2013.1.01596.S (Goddi et al. 2018) observed band 6 (1 mm, SiO J=5-4), 2017.1.00293.S observed Band 3 (3 mm, CS J=2-1), and the Karl G. Jansky Very Large Array (VLA) program VLA 16B-202 observed Q-band (7 mm, CS J=1-0). The ALMA data were taken in long-baseline configurations, and the VLA data were taken in the most extended configuration (A).

For the ALMA data, both at 1 mm and 3 mm, we use the pipeline-produced calibrated data for the emission line maps. The Band 6 (1 mm) continuum data were self-calibrated as described in Goddi et al. (2018), using nine iterations of phase-only self-calibration; the solutions were only used for the continuum data.

The VLA data were calibrated with the EVLA pipeline¹ with radio frequency interference (RFI) flagging and Hanning smoothing disabled to avoid flagging bright lines.

We imaged the CS J=2-1 line at 97.980953 GHz with robust 0.5 weighting with 3 km s⁻¹ channels, resulting in a beam 0.067'' × 0.043'', PA=-44.5°, and sensitivity $\sigma_{rms} = 0.59$ mJy beam⁻¹ (26 K). The CS J=1-0 line at 48.990955 GHz was included in a continuum band with 6 km s⁻¹ resolution, and we imaged it with robust 0 weighting, resulting in a beam 0.043'' × 0.037'', PA=-64.8° and sensitivity 1.3 mJy beam⁻¹ (420 K). We also imaged the CS v=1 J=1-0 line at the same resolution with a sensitivity of $\sigma_{rms} = 1.1$ mJy beam⁻¹ (350 K), but did not detect it. The SiO J=5-4 and J=2-1 lines and band 6 (1 mm) continuum were imaged with robust 0.5 weighting with beam sizes 0.041'' × 0.035'', PA=-44.8° and 0.079'' × 0.053'', PA=-42.8°, respectively.

The VLA and ALMA data used the same phase calibrator, J1922+1530, with coordinates that differ by 0.003'' mostly in RA. Both the VLA and ALMA positions are offset from the SIMBAD position by about 0.0015''. The VLA measurement set data incorrectly report the stored coordinate for J1922+1530 as being in the FK5 system, while the ALMA measurement sets correctly report the stored coordinate as being in ICRS. The difference between the ICRS and FK5 system is about 0.03'' at this position, close to the beam size, and therefore is highly relevant for these data. We corrected the images for the coordinate system offset (0.03''), but did not correct for the $\approx 0.003''$ discrepancy in calibrator position, so our systematic pointing error is approximately 0.003'' (16 AU).

We report a check on the velocity frame and a search for variability in the Appendices.

3. RESULTS

We report the detection of two transitions of CS, J=2-1 and J=1-0, with peak brightness $T_{B,max} \approx 7000$ K. These lines peak at different locations both spatially (Figure 1) and spectrally (Figure 2). We report Gaussian fit parameters to the line profiles and to the peak intensity images in Table 1; the errors reported in the table are fit errors assuming no correlation between the parameters, and they do not include the systematic pointing uncertainty noted in Section 2.

The CS J=2-1 line is observed in the blueshifted component of the previously-detected SiO outflow (Goddi et al. 2018). It has both a compact component, which we will refer to as the CS 2-1 maser, and an extended com-

ponent that traces the inner envelope of the blueshifted outflow. This extended component can be seen more clearly in the 42 km s⁻¹ channel of the channel maps (Figure 3). The maser peak is located at the base of the blueshifted outflow (Figure 1) at a velocity of $v_{lsr} = 34.50 \pm 0.07$ km s⁻¹.

The CS J=1-0 line is only seen as a single spatial component centered at approximately $v_{lsr} = 64 \pm 6$ km s⁻¹. It is centered closer to the central continuum source, but still slightly toward the blueshifted outflow. The CS J=1-0 and J=2-1 masers are offset by $0.036'' \pm 0.12''$ (190 ± 60 AU).

4. ANALYSIS

The peak brightness of the observed lines is ~ 6800 K at $\sim 0.07''$ (350 AU at 3 mm) and $\sim 0.04''$ (200 AU at 7 mm) resolution. It is unlikely that the molecules are in thermal equilibrium at $T_K \geq 6000$ K, since such high temperatures would more likely result in dissociation of the molecules (e.g., Pattillo et al. 2018).

At the observed spectral resolution of 3 km s⁻¹, the CS J=2-1 line is marginally resolved with FWHM = 5.25 km s⁻¹ ($\sigma = 2.2$ km s⁻¹), and at 6 km s⁻¹ resolution, the CS J=1-0 line is unresolved. The thermal line width of CS at 6000 K is FWHM = 2.7 km s⁻¹ ($\sigma = 1.1$ km s⁻¹), smaller than the measured width of CS J=2-1 and smaller than the resolution of the CS J=1-0 data. Lines narrower than their thermal width are a clear indication of maser emission (Elitzur 1982), but our observations have too coarse resolution to identify such narrow widths if they are present.

The high observed brightness temperature is partial evidence that these transitions are masing. The locations of the emission features provides additional and definitive evidence that they are masing. The emission peaks are at clearly different velocities and they may be from different spatial locations (separated by about 190 AU). They are therefore not emitted by the same material. This velocity difference rules out a thermal origin for either transition, since thermal lines should have comparable brightness in both transitions at similar velocities.

The separation between the two maser spots in position and velocity hints that the masers could be produced at the extreme ends of a disk orbiting a central protostar. If we assume the masers trace orbiting material, their velocity and spatial separation can be used to infer the central source mass. At a separation of 30 km s⁻¹ and 190 AU, assuming the masers come from opposite ends of a disk such that $v_{orb} = 15 \pm 1$ km s⁻¹ and $R_{disk} = 95 \pm 30$ AU, the implied contained mass is $M = 24_{-10}^{+12} M_{\odot}$. This mass is comparable to that

¹<https://science.nrao.edu/facilities/vla/data-processing/pipeline>

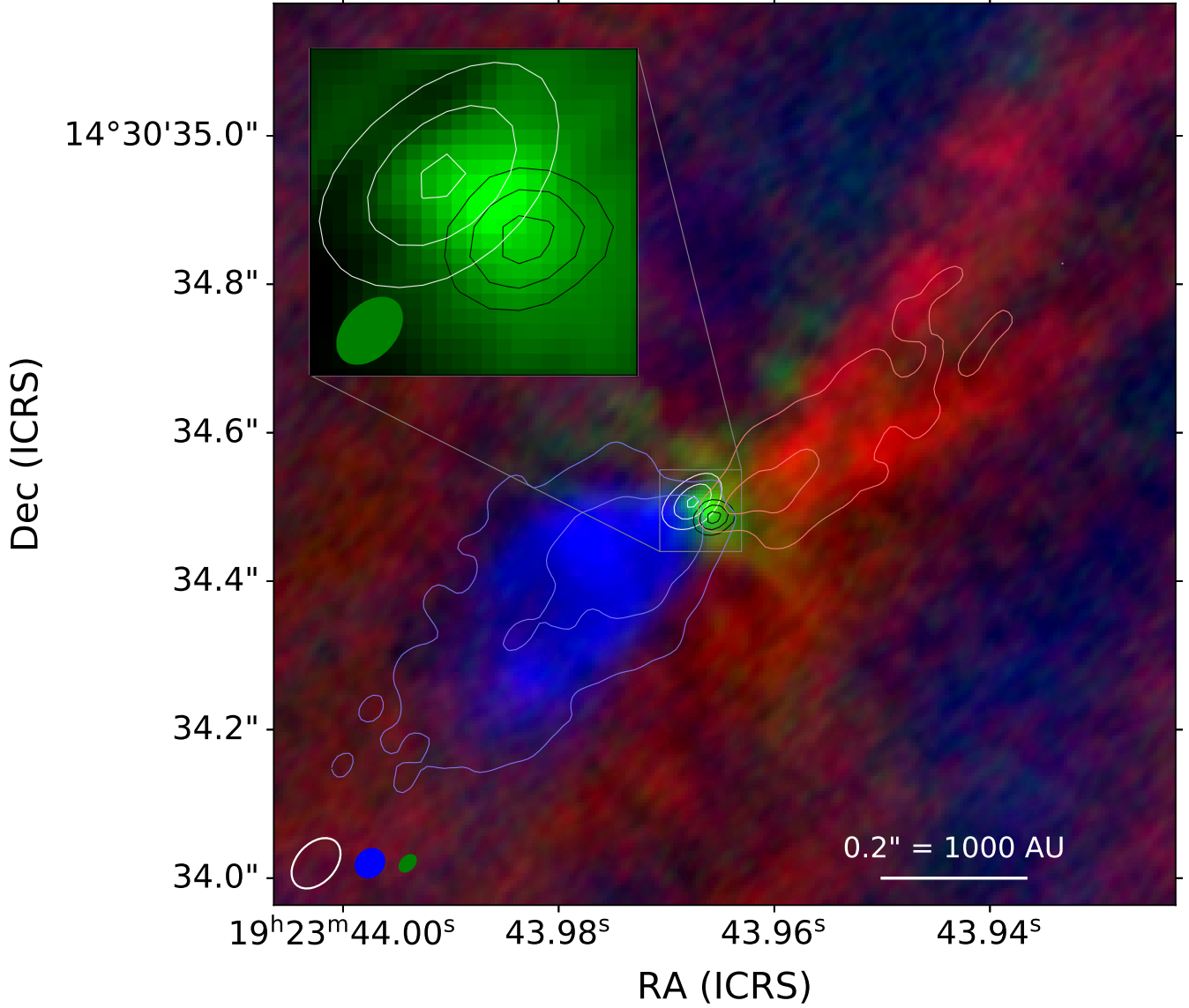


Figure 1. An image of the SiO J=5-4 outflow (red and blue corresponding to red and blueshifted emission integrated over 74-118 km s^{-1} and -32 to 55 km s^{-1} , respectively) with 1 mm continuum shown in green. The contours show integrated SiO J=2-1 over the same ranges in red (0.05, 0.1 K km s^{-1}) and blue (0.1, 0.2 K km s^{-1}), the CS 2-1 maser in white (2000, 4000, 6000 K peak intensity at 34.5 km s^{-1}), and the CS 1-0 maser in black (2000, 4000, 6000 K peak intensity at $\sim 65.5 \text{ km s}^{-1}$). For each of the masers, the contours effectively indicate the synthesized beam size. The white, blue, and green ellipses in the bottom left show the synthesized beam sizes of the SiO J=2-1, SiO J=5-4, and 1 mm continuum images, respectively. The inset image shows only the continuum and the maser contours, but is otherwise identical.

Table 1. Line Fit Parameters

Line Name	Amplitude (K)	v_{LSR} (km s^{-1})	σ_{FWHM} (km s^{-1})	RA (ICRS) (deg)	Dec (ICRS) (deg)
CS J=1-0	6800	64 ± 6	7.3 ± 1.2	$290.9331902 \pm 0.0000025$	14.5095795 ± 0.0000021
CS J=2-1	6700 ± 200	34.50 ± 0.07	5.27 ± 0.17	$290.9331982 \pm 0.0000025$	14.5095852 ± 0.0000021

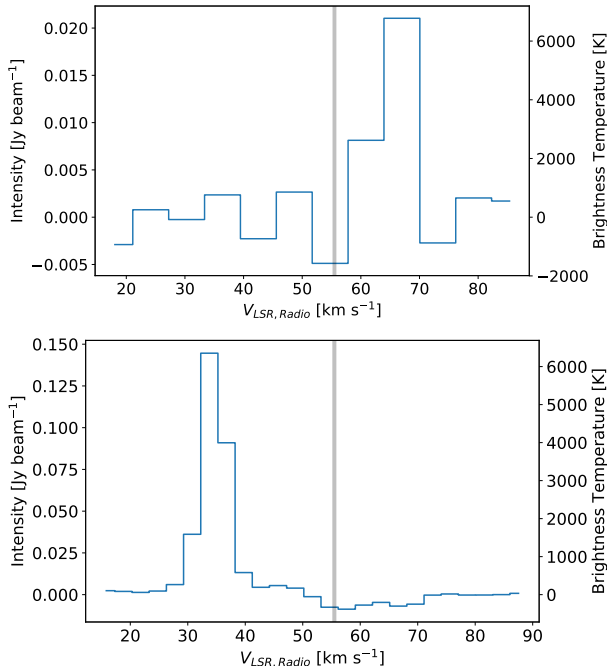


Figure 2. Plots of the (a) CS J=1-0 and (b) CS J=2-1 spectra toward their respective peak locations shown in Figure 1. The vertical line shows the estimated velocity of W51 e2e from the NH₃ inversion lines at 56.4 km s⁻¹ (Goddi et al. 2016, Table 4).

suggested by Ginsburg et al. (2017) and Goddi et al. (2018) based on luminosity estimates. However, the velocity separation also hints that these masers may be produced in the outflow rather than in a disk. In that case, the orbital analysis is not valid.

Our data also include the W51 IRS2/North and W51 e8 high-mass young stellar objects (HMYSOs) (Ginsburg et al. 2017). No compact and bright CS emission sources were detected toward either of these HMYSO candidates, with a peak CS 2-1 flux limit $S_{98\text{GHz}} \leq 15\text{mJy beam}^{-1}$, an order of magnitude fainter than the peaks seen in W51 e2e. However, plentiful extended CS 2-1 emission is seen around each of the HMYSOs. This difference indicates that there is something unique about the chemistry, geometry, or excitation in the W51 e2e that drives these particular maser transitions.

The detection of CS 1-0 emission at ~ 65 km s⁻¹ is actually quite surprising, since W51 e2e is deeply embedded in a high column density molecular medium that covers this velocity. Since the maser is detected, there must either be a hole in the cloud through which we are seeing the compact emission, or the foreground cloud’s CS is highly excited and has a minimal ground-state population at 65 km s⁻¹. The J=2-1 transition at 34.5 km s⁻¹ is not subject to this concern, since there is no

foreground material at that velocity, but it is possible that a 2-1 maser exists near 65 km s⁻¹ and is fully absorbed by foreground cloud material.

Masers from CS have been predicted in the atmospheres of evolved stars. Schoenberg (1988) used an expanding shell model appropriate to evolved stars in which temperature, density, and velocity are all decreasing with radius corresponding to some mass loss rate and terminal wind velocity. They predict masing in the CS J=1-0 and J=2-1 lines under different conditions, though the masing is fairly weak (factors of a few). In these models, the stellar infrared radiation drives the maser. The similarity between the atmospheres of evolved stars and the innermost regions around accreting high-mass stars hints that these maser models may apply in both environments.

Finally, we note that no other masers detected in the region coincide with the CS masers. The closest OH and water masers (Fish & Reid 2007; Sato et al. 2010) are separated by $> 0.2''$ (> 1000 AU). There are some CH₃OH maser spots with positions close to W51e2e’s core (~ 350 AU, $0.07''$) and with the CS masers at a velocity ~ 60 km s⁻¹, but they are not co-located (Etoke et al. 2012; Surcis et al. 2012). No other known masers are clearly emitted from the same positions as the CS masers. Appendix C shows maser locations overlaid on Figure 1.

5. CONCLUSIONS

We have detected two emission lines from the J=2-1 and J=1-0 transitions of CS with high brightness temperature (≥ 6800 K) indicating that these lines are masers. This is the first reported detection of maser emission from CS. While the HMYSO W51 e2e exhibits these masers, several neighboring HMYSOs that are similar in luminosity, core mass, and apparent evolutionary stage do not. The presence of two CS masers from different rotational states at different velocities and locations in one source, W51 e2e, combined with the absence of either of these masers in the other HMYSOs in the region, W51 IRS2/North and W51 e8, suggests that there is something unique about W51 e2e’s radiation field, geometry, or chemistry that promotes CS maser formation.

These CS masers join a growing list of rarely-detected maser transitions that may trace a unique phase in the formation of high-mass protostars. Like the NH₃, H₂CO, and SiO masers, there are only 1-10 known sources of each of these masers. Curiously, W51 IRS2/North, a known host of NH₃ and SiO masers, does not exhibit any CS maser emission. Other HMYSOs should be searched for masers in these transitions to

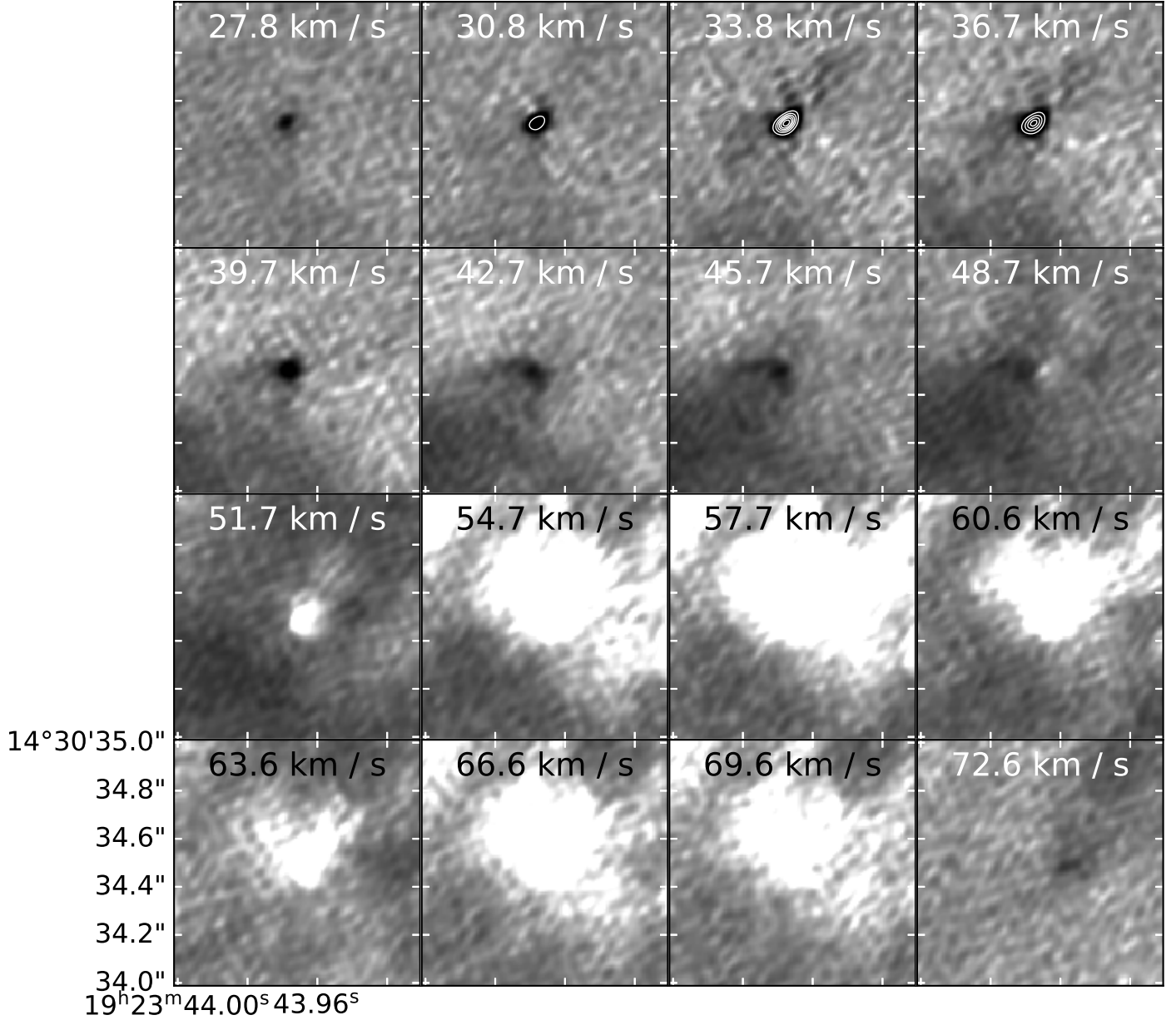


Figure 3. Continuum-subtracted channel maps of the CS J=2-1 transition. Channels are 3 km s^{-1} wide. Darker colors indicate higher intensity. White contours are overlaid at $[0.02, 0.04, 0.06, 0.08, 0.1, 0.125] \text{ Jy beam}^{-1}$. Absorption from the foreground against the continuum is shown as negative intensity (white) from 50-70 km s^{-1} . The redshifted outflow is faint but still detected at $\sim 72.5 \text{ km s}^{-1}$.

determine how common they are and precisely what evolutionary stage they trace.

Acknowledgements We thank Todd Hunter for providing literature references on CS masers and Lorant Sjouwerman for discussion about a lack of CS masers in AGB stars. We thank the anonymous referee for a helpful review.

This paper makes use of the following ALMA data sets: ADS/JAO.ALMA#2013.1.01596.S and 2017.1.00293.S. ALMA is a partnership of ESO (rep-

resenting its member states), NSF (USA) and NINS (Japan), together with NRC (Canada), MOST and ASIAA (Taiwan), and KASI (Republic of Korea), in cooperation with the Republic of Chile. The Joint ALMA Observatory is operated by ESO, AUI/NRAO and NAOJ. The National Radio Astronomy Observatory is a facility of the National Science Foundation operated under cooperative agreement by Associated Universities, Inc.

Software This paper used `astropy` (Astropy Collaboration et al. 2013, 2018), `pyspeckit` (Ginsburg & Mirocha 2011), and `CASA` (McMullin et al. 2007).

APPENDIX

A. VELOCITY CHECK

We carefully checked the velocity measurements in the VLA data, since an offset of a few channels is comparable to the Earth’s motion and we are using a continuum band to infer velocity information. The observations we analyze were taken on December 26 and 30, 2016 and January 7, 2017. On these dates, the topocentric-to-barycentric velocity corrections are -9.0 , -7.4 , and -4.1 km s^{-1} , respectively. The barycentric-to-LSR correction toward W51 is 16.5 km s^{-1} . The observed CS $J=1-0$ peak is in channel 24 (zero-indexed) of spectral window 26, which has channel 0 at 48957.667, 48957.932, and 48958.478 MHz, respectively, for each of the three observations. The channel width is 1 MHz. The LSR velocity of the CS $J=1-0$ peak intensity channel is at 64.3 km s^{-1} on all three dates. This value is consistent with our reported velocity of $v_{LSR}(\text{CS } J=1-0) = 65.5 \pm 0.7 \text{ km s}^{-1}$.

No such sanity check is needed for the ALMA data, since the channel maps clearly show the outflow at appropriate velocities with morphology that matches the SiO outflow seen at both 1 mm and 3 mm.

B. VARIABILITY CHECK

We also checked for variability in the CS 1-0 maser, and found no evidence for variability across four observing epochs (2016-10-02, 2016-12-26, 2016-12-30, 2017-01-07; the former was not included in our merged data set because we were unable to perform bandpass calibration). The position remained constant and the flux remained consistent to within single-epoch observing errors.

C. ADDITIONAL FIGURES SHOWING OTHER MASER LOCATIONS

We show Figure 1 with maser positions from CH_3OH , OH, and H_2O (Fig. 4) in this Appendix. These figures highlight that the conditions to excite each of these masers is unique.

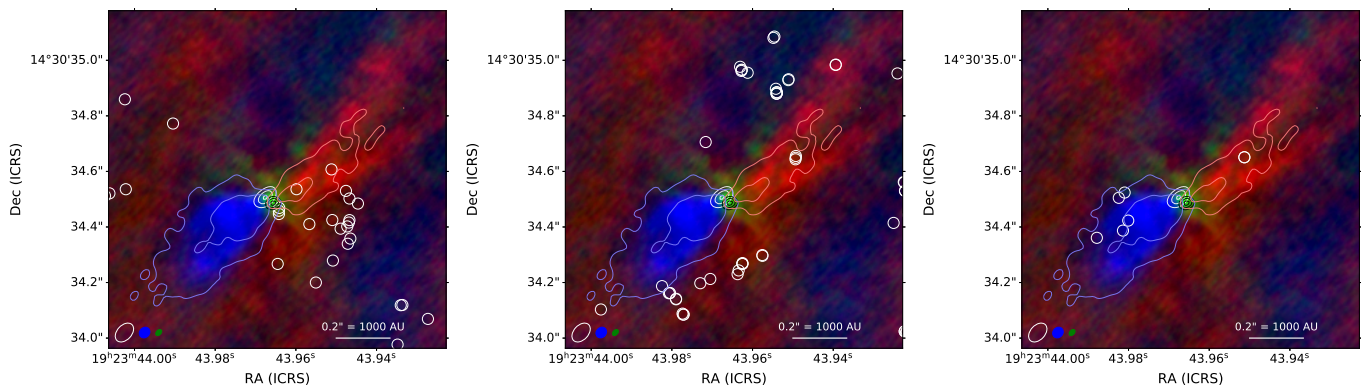


Figure 4. Figure 1 reproduced with (a) CH_3OH maser spots from Etoka et al. (2012), (b) OH maser spots from Fish & Reid (2007), and (c) H_2O maser spots from Sato et al. (2010) overlaid.

REFERENCES

- Araya, E. D., Olmi, L., Morales Ortiz, J., et al. 2015, *ApJS*, 221, 10
- Astropy Collaboration, Robitaille, T. P., Tollerud, E. J., et al. 2013, *A&A*, 558, A33
- Astropy Collaboration, Price-Whelan, A. M., Sipőcz, B. M., et al. 2018, *AJ*, 156, 123
- Cho, S.-H., Yun, Y., Kim, J., et al. 2016, *ApJ*, 826, 157
- Cordiner, M. A., Boogert, A. C. A., Charnley, S. B., et al. 2016, *ApJ*, 828, 51

- Eisner, J. A., Greenhill, L. J., Herrnstein, J. R., Moran, J. M., & Menten, K. M. 2002, *ApJ*, 569, 334
- Elitzur, M. 1982, *ApJ*, 262, 189
- Etoka, S., Gray, M. D., & Fuller, G. A. 2012, *MNRAS*, 423, 647
- Fish, V. L., & Reid, M. J. 2007, *ApJ*, 670, 1159
- Ginsburg, A. 2017, ArXiv e-prints, arXiv:1702.06627
- Ginsburg, A., Bally, J., Battersby, C., et al. 2015, *A&A*, 573, A106
- Ginsburg, A., & Mirocha, J. 2011, PySpecKit: Python Spectroscopic Toolkit, Astrophysics Source Code Library, , ascl:1109.001
- Ginsburg, A., Goddi, C., Kruijssen, J. M. D., et al. 2017, *ApJ*, 842, 92
- Goddi, C., Ginsburg, A., Maud, L., Zhang, Q., & Zapata, L. 2018, ArXiv e-prints, arXiv:1805.05364
- Goddi, C., Ginsburg, A., & Zhang, Q. 2016, *A&A*, 589, A44
- Goddi, C., Greenhill, L. J., Chandler, C. J., et al. 2009, *ApJ*, 698, 1165
- Goddi, C., Henkel, C., Zhang, Q., Zapata, L., & Wilson, T. L. 2015, *A&A*, 573, A109
- Goddi, C., Moscadelli, L., & Sanna, A. 2011, *A&A*, 535, L8
- Hasegawa, T., Morita, K., Okumura, S., et al. 1986, in *Masers, Molecules, and Mass Outflows in Star Formation Regions*, ed. A. D. Haschick, 275
- Henkel, C., Wilson, T. L., Asiri, H., & Mauersberger, R. 2013, *A&A*, 549, A90
- Highberger, J. L., Apponi, A. J., Bieging, J. H., Ziurys, L. M., & Mangum, J. G. 2000, *ApJ*, 544, 881
- Hofner, P., Kurtz, S., Churchwell, E., Walmsley, C. M., & Cesaroni, R. 1994, *ApJL*, 429, L85
- Matthews, L. D., Greenhill, L. J., Goddi, C., et al. 2010, *ApJ*, 708, 80
- McMullin, J. P., Waters, B., Schiebel, D., Young, W., & Golap, K. 2007, in *Astronomical Society of the Pacific Conference Series*, Vol. 376, *Astronomical Data Analysis Software and Systems XVI*, ed. R. A. Shaw, F. Hill, & D. J. Bell, 127
- Mills, E. A. C., Ginsburg, A., Clements, A. R., et al. 2018, *ApJL*, 869, L14
- Moscadelli, L., & Goddi, C. 2014, *A&A*, 566, A150
- Moscadelli, L., Sánchez-Monge, Á., Goddi, C., et al. 2016, *A&A*, 585, A71
- Pattillo, R. J., Cieszewski, R., Stancil, P. C., et al. 2018, *ApJ*, 858, 10
- Sato, M., Reid, M. J., Brunthaler, A., & Menten, K. M. 2010, *ApJ*, 720, 1055
- Schoenberg, K. 1988, *A&A*, 195, 198
- Surcis, G., Vlemmings, W. H. T., van Langevelde, H. J., & Hutawarakorn Kramer, B. 2012, *A&A*, 541, A47
- Wilson, T. L., & Schilke, P. 1993, in *Lecture Notes in Physics*, Berlin Springer Verlag, Vol. 412, *Astrophysical Masers*, ed. A. W. Clegg & G. E. Nedoluha, 123–126